Author Queries

Journal: Journal of the Royal Society Interface

Manuscript: rsif20170036

As the publishing schedule is strict, please note that this might be the only stage at which you are able to thoroughly review your paper.

Please pay special attention to author names, affiliations and contact details, and figures, tables and their captions.

The corresponding author must provide an ORCID ID if they haven't done so already. If you or your co-authors have an ORCID ID please supply this with your corrections. More information about ORCID can be found at http://orcid.org/.

No changes can be made after publication.

SQ1 Your supplementary material will be published online alongside your article and on rs.figshare.com exactly as the file(s) are provided. Therefore, please could you either confirm that your supplementary material is correct, or – if you have any changes to make to these files – email these along with your proof corrections to the journal inbox. Your ESM files are listed here for your convenience:

Supp1.tif

Supp2.jpg

Q1 Please check whether the edits made to the article title are okay.

Q2 Please check hierarchy of the headings.

Q3 Please provide the year for 'G. T. Reels, personal communication'

Q4 Reference [17] has been repeated and hence the repeated version has been deleted. Please check.

Q5 Please update reference [45].

Q6 Please supply the page range in the reference [58].

Q7 Please note that the captions of figures 1–4 have been taken from the metadata.

INTERFACE

rsif.royalsocietypublishing.org

Research

Cite this article: Nixon MR, Orr AG, Vukusic P. 2017 Covert linear polarization signatures from brilliant white two-dimensional disordered wing structures of the phoenix damselfly. *J. R. Soc. Interface* 20170036. http://dx.doi.org/10.1098/rsif.2017.0036

Received: 19 January 2017
Accepted: 8 May 2017

Subject Category:
Life Sciences–Physics interface

Subject Areas:
biophysics, biomaterials

Keywords:
structural colour, whiteness, polarization, *Pseudolestes mirabilis*, Odonata

Authors for correspondence:
M. R. Nixon
e-mail: m.r.nixon@exeter.ac.uk
P. Vukusic
e-mail: p.vukusic@exeter.ac.uk

Electronic supplementary material is available online at rs.figshare.com.

THE ROYAL SOCIETY PUBLISHING

Covert linear polarization signatures from brilliant white two-dimensional disordered wing structures of the phoenix damselfly

M. R. Nixon[1], A. G. Orr[2] and P. Vukusic[1]

[1]School of Physics, University of Exeter, Exeter EX4 4QL, UK
[2]Environmental Futures Centre, Griffith University, Nathan, Q4111, Australia

MRN, 0000-0002-6351-4223

The damselfly *Pseudolestes mirabilis* reflects brilliant white on the ventral side of its hindwings and a copper-gold colour on the dorsal side. Unlike many previous investigations of odonate wings, in which colour appearances arise either from multilayer interference or wing-membrane pigmentation, the whiteness on the wings of *P. mirabilis* results from light scattered by a specialized arrangement of flattened waxy fibres and the copper-gold colour is produced by pigment-based filtering of this light scatter. The waxy fibres responsible for this optical signature effectively form a structure that is disordered in two-dimensions and this also gives rise to distinct optical linear polarization. It is a structure that provides a mechanism enabling *P. mirabilis* to display its bright wing colours efficiently for territorial signalling, both passively while perched, in which the sunlit copper-gold upperside is presented against a highly contrasting background of foliage, and actively in territorial contests in which the white underside is also presented. It also offers a template for biomimetic high-intensity broadband reflectors that have a pronounced polarization signature.

1. Introduction

There are many examples of sub-micron-sized structures in nature that give rise to reflected colour in both flora and fauna [1–7]. Often this results in bright, iridescent colour and a highly conspicuous appearance. In many cases, structural colour has been linked to significant biological functions such as territorial and courtship signalling [8,9], and to less conspicuous colouring for camouflage [10,11]. Insects, in particular, are an especially diverse class, within which a wide range of different mechanisms of colour-production have been elucidated [4]. Various species of the butterfly genus *Morpho* exhibit a brilliant blue appearance generated by the 'Christmas-tree' shaped ridge-lamellae on their wing-scales [12–14]. Similarly, many species of Coleoptera reflect bright colours from multi-layered structures in their elytra [15–17], some also displaying circular dichroism, leading to strongly circularly polarized coloured reflections [18–21]. In several species of Lepidoptera natural, multi-domained gyroid-type three-dimensional photonic crystals (PCs) have been found. These give rise to the diffuse green regions of colour in such species as *Callophrys rubi* [22] and *Parides sesostris* [23–25].

Colour-inducing structure also occurs in the wing membranes [15,26–31] and bodies [32] of some species of *Odonata*. In all species thus far examined the wing membranes exhibit bright iridescence arising from multilayer-type interference. Moreover in various odonates low intensity white pruinescence has been attributed to scattering of incident light by wax crystals secreted by the epicuticle of the wing membrane or the body [28,33], but these cases involve relatively simple structures and low levels of reflectance. By contrast, *Pseudolestes mirabilis* (commonly known as the Phoenix damselfly), the subject

of this investigation, exhibits a significantly different photonic structure from any previously reported in Odonata and this structure creates brilliant whiteness. Structural white in nature is normally achieved via the random scattering of incident light from disordered structures, such as the filamental arrangement in *Cyphochilus* [34] and other species of beetle [35,36]. Further examples of biological structures that produce a bright white appearance include the dense arrays of pterin pigments in pierid butterflies [37,38], the disordered arrangement of guanine crystals in the *Latrodectus pallidus* spider [39] and the leucophore cells in the flexible skin of cuttlefish (*Sepia officinalis*) [40]. The *P. mirabilis* system differs from all previous examples of structural whiteness in the Animal Kingdom. To our knowledge, it is the first reported example of an animal with a disordered two-dimensional scattering structure.

2. Methods

2.1. Materials

Specimens of *Pseudolestes mirabilis* Kirby 1900 (Insecta: Odonata: Pseudolestidae), a taxonomically isolated stream dwelling damselfly endemic to Hainan island, were collected in the field, killed and fixed in acetone: 2 m# fully mature imagines; Wuzhishan, Hainan Province, P.R. of China, 16-iv-2008, collector unknown. Deposited in collection A.G. Orr, Caloundra, Queensland, Australia.

2.1.1. Optical microscope imaging

Optical microscopy was carried out in dark-field epi-illumination and trans-illumination using a Zeiss Axioscope 2 with objective lenses providing a range of magnifications. Images were captured using a Zeiss Axiocam MRc5 camera.

2.1.2. Scanning electron microscopy imaging

Scanning electron microscopy (SEM) images were acquired using a Nova 600 NanoLab Dualbeam system. Samples were cut from the wings of *P. mirabilis*, with a typical size of approximately 10 mm^2. These were mounted on an SEM stub with electrically conducting epoxy resin and sputter coated with approximately 5 nm AuPd then examined using an electron beam voltage of 10 kV, beam current of 7.5 pA and a working distance of 5 mm.

2.1.3. Focused ion beam milling

Focused ion beam (FIB) milling of regions through the *P. mirabilis* photonic structure was achieved with the previously described Nova 600 NanoLab Dual-beam system and the same sample prepared for SEM imaging. A suitable region of the sample was identified (namely an undamaged region of the fibre-structure) using the electron beam and aligned so that the region to be milled was perpendicular to the fibres. To mill the rectangular section, a beam voltage of 30 kV and a beam current of 1 nA was used at a working distance of 5 mm.

2.1.4. Reflection spectrometry

Reflection spectrometry was carried out with an Ocean Optics ISP-50-8-R-GT integrating sphere (ISP). Light was incident from a 1000 µm optical fibre connected to an Ocean Optics HPX-2000 high-power Xenon light-source. After passing through a pinhole and undergoing collimation by a lens, incident light was polarized in either a parallel or perpendicular state. This was then focused through an integrating sphere to a beam spot with a diameter of approximately 1.5 mm coincident with the sample (located at the far side of the ISP). The reflected scatter from the sample was captured by the ISP before being delivered to an Ocean Optics USB2000+ high-resolution USB spectrometer via a 1000 µm optical fibre. The measured reflectance was normalized against the reflectance from an Ocean Optics WS-1 white reflectance standard.

2.1.5. Imaging scatterometry

Imaging scatterometry was undertaken using a standard protocol (details of which can be found in Stavenga *et al.* (2009) [41] and Vukusic and Stavenga (2009) [42]). Narrow-angle ('primary beam') illumination was used to illuminate a single-cell region of wing-membrane and covering fibres. A wing piece was mounted on a pulled glass pipette using a small amount of quick-setting epoxy resin.

2.1.6. Finite-difference time-domain modelling

The electromagnetic response of the binary images of the structure's cross-section (e.g. Figure 4) was computed with Lumerical FDTD Solutions v. 8.12 (https://www.lumerical.com/tcad-products/fdtd/). The structure at the two end-edges of the binary images (to within less than 1 µm from the structure edge) were marginally realigned so as to be identical to one another, thus allowing a set of periodic boundary conditions to be applied to the modelling unit cell with no discontinuities across the unit cell structure's edges. This effectively uses the 50 µm binary image as a unit cell, creating an infinitely repeating structure in the plane (the *x*-axis, in conventional notation). Perfectly matched layer boundaries were applied to the top and bottom of the simulation region to absorb radiation incident at these locations. A plane-wave pulse of incident 400–700 nm electromagnetic radiation was introduced to the simulation and the frequency-domain reflectance response was calculated from the power transmitted across a boundary located above the incident wave source. A value of 1.38 was used for the fibres' refractive index (based on values determined for effective refractive indices of wax layers with rough surface in previous studies [29,31,43]).

3. Results

The hind-wings of mature male *P. mirabilis* have a highly-visible bright-white patch on their ventral sides (figure 1*a*,*b*) which is displayed to rival males during agonistic displays contesting territory [44]. Examination of this region with an optical microscope reveals that the white appearance originates from an epicuticular wax secretion formed from flattened parallel fibres which are extruded from the faces of the cross veins on either side of the wing cells, such that they eventually meet in the middle of the cell and interknit [45] (figure 1*c*). This wax is considered homologous with that associated with diffuse white pruinescence occurring widely in Odonata [46,47]. The dark-field image of the edge of a white region in figure 1*c* shows that the secreted fibrous structure diffusely scatters white light over a range of incident angles. Fractured edge-regions of the white area, appear to also show that the structure has directionality, namely, the small strands and fractured regions of the structure can be seen occupying a direction parallel to the axial veins defining each wing-cell (in figure 1*c*).

Closer inspection of the white region using SEM reveals that these strands comprise many individual, aligned fibres. Figure 1*d* shows a macroscopic top-down view of fibres across a wing cell, while figure 1*e* shows the fractured edges of two layers of fibres. These fibres appear to extend from the cross-veins located at the longitudinal edges of

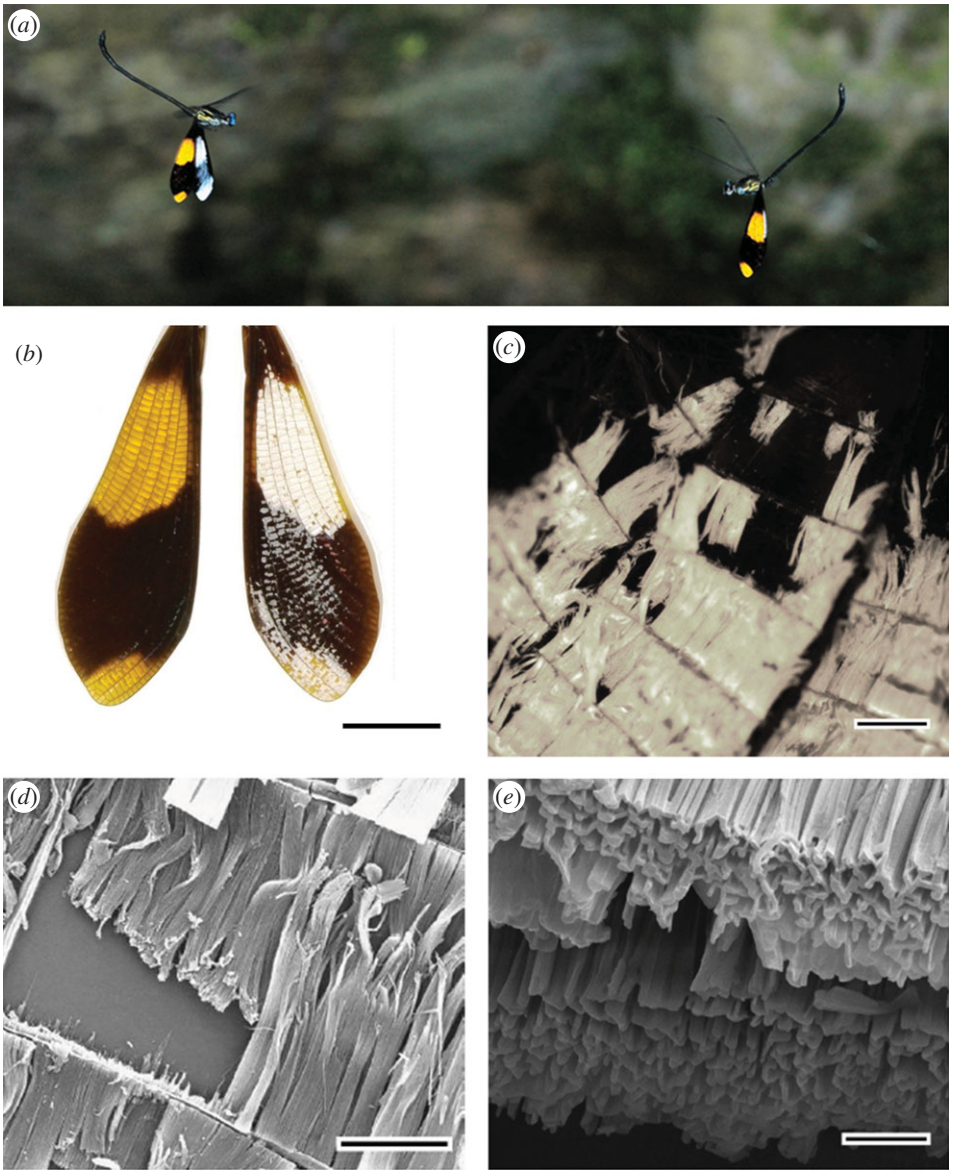

Figure 1. Images of the *Pseudolestes mirabilis* damselfly: (*a*) Photograph of two *P. mirabilis* males in agonistic display, courtesy of G. T. Reels (cropped version of original image). (*b*) Images of the dorsal (left) and ventral (right) sides of an individual *P. mirabilis* hind-wing. (*c*) Dark-field epi-illumination optical microscope image of a several-cell region of the ventral side of a *P. mirabilis* hind-wing at the edge of a fibre-covered wing-membrane region. (*d*) An SEM image of an entire wing-cell region, showing the extracellular fibre structure. (*e*) A higher-magnification SEM image of a naturally fractured region of fibres, showing the exposed structure cross-section. Scale bars: (*b*) 5 mm; (*c*) 200 µm; (*d*) 150 µm; and (*e*) 3 µm.

individual wing cells (i.e. discrete regions of wing membrane enclosed by veins). The SEM image in figure 1*e* shows a naturally fractured edge of a strand of fibres. Here, irregular cross-sections can be seen in the air pockets that are created in the inter-fibre regions. These cross-sections show no discernible order on length scales associated with optical scattering, as determined by Fast Fourier Transform (FFT) analysis—see electronic supplementary material, S1.

This controlled directionality of the fibre-structure confers a distinct linear polarization signature to the wings, an optical feature observable as a difference in reflectance between incident orthogonal linear polarizations as can be seen from the measurements presented in figure 2. For the white wing region on the ventral side of the *P. mirabilis* hind-wing, figure 2*c* shows that the average measured reflectance across visible wavelengths is 58% for light polarized with its ***E***-field vector parallel to the structure's strands (referred to here as *parallel polarization*), whereas for perpendicular polarization this intensity is only 47%. This equates to an average degree of polarization of 0.1 across all visible wavelengths, where degree of polarization (P) is defined by the equation:

$$P = \frac{R_{\text{para}} - R_{\text{perp}}}{R_{\text{para}} + R_{\text{perp}}} \tag{3.1}$$

and R_{par} and R_{perp} are the reflected intensity from light incident in parallel and perpendicular polarization configurations, respectively. The 0.1 degree of polarization for this system is equivalent to a 19% proportional decrease in reflectance (i.e. an absolute difference of 11%) for incident light with parallel polarization compared to perpendicular polarization.

For both incident light polarizations the spectral reflectance is relatively flat and 'feature-free', albeit with a slight increase in intensity towards shorter wavelengths. The measured reflectance from the white area equates to CIE*Lab* a^* values of 1.3 and 1.1, and b^* values of −8.0, and −8.2 for parallel and perpendicular polarizations, respectively. These scores correspond to very low levels of colour-

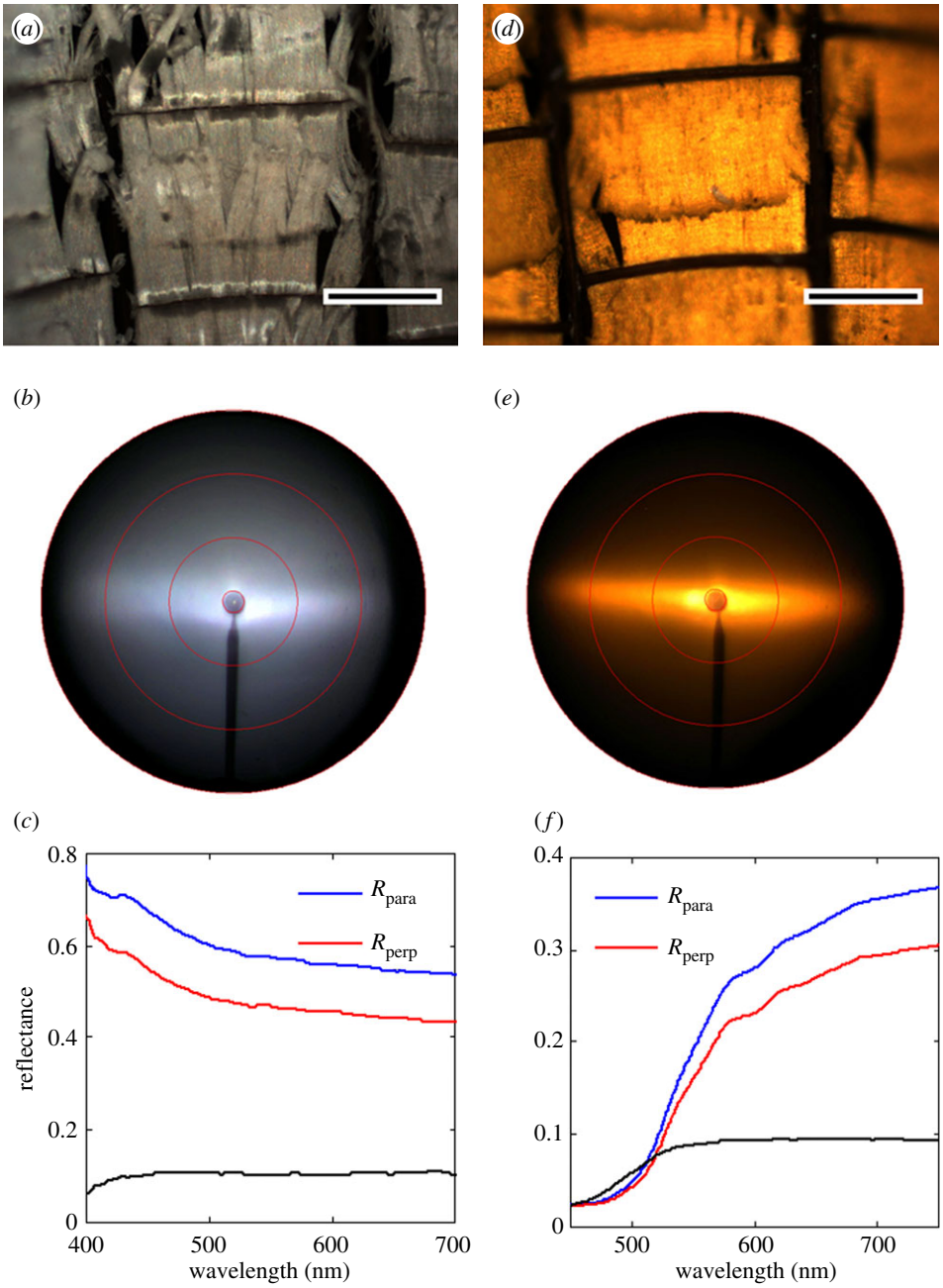

Figure 2. (*a*) Optical microscope image of the ventral side of the *Pseudolestes mirabilis* hindwing (*b*) Scattergram of an individual *P. mirabilis* fibre-covered wing-cell; the sample was mounted with the fibres aligned vertically. The red lines are added to show scattered angles of 5°, 30°, 50° and 90°. (*c*) Integrating-sphere-measured reflectance from the white region on the ventral side of a *P. mirabilis* hind-wing, for incident light with parallel polarization (blue lines) and perpendicular polarization (red line). The corresponding degree of polarization is shown by the black line. (*d*–*f*) are equivalent measurements from the dorsal side of the same region as used for (*a*–*c*). Scale bars in (*a*) and (*d*) both 200 µm. Q7

saturation. This reflected scatter extends to approximately 70° in the plane perpendicular to the fibre direction as shown in the scattergram image in figure 2*b*.

The brilliant copper-gold colour of the dorsal side of the hindwings exhibits the same polarization characteristics as the ventral (white) side (figure 2*e*). The intensity of the copper-gold dorsal reflectance is, however, significantly lower than that of the white ventral reflectance, especially at shorter wavelengths (figure 2*f*). The spectral shape of the transmittance taken through the pigmented region of wing fits closely to that associated with melanin [48] (figure 3). This strongly suggests the copper-gold dorsal colour is produced by the spectral filtering of light travelling through the wing membrane after first having been reflected from the fibre-structure.

To understand more clearly the reflection properties of the fibrous structure we performed FIB-milling to obtain a large cross-section through the fibres. We used an SEM image of the section (figure 4*a*) to create a two-dimensional binary representation, appropriately correcting for non-normal imaging angles. This representation was used in a finite-difference time-domain (FDTD) simulation of the structure's optical response to incident polarized light. Equivalent simulations were also undertaken for fibre-structures with different filling fractions, generated by digitally modifying the sizes of the air-pocket regions in the binary image of the *P. mirabilis* photonic structure, while keeping their positions, shapes and the thickness of the entire structure, constant (figure 4*b*).

The FDTD-modelled original (*P. mirabilis*) and filling-fraction-altered structures (figure 4) all show the same

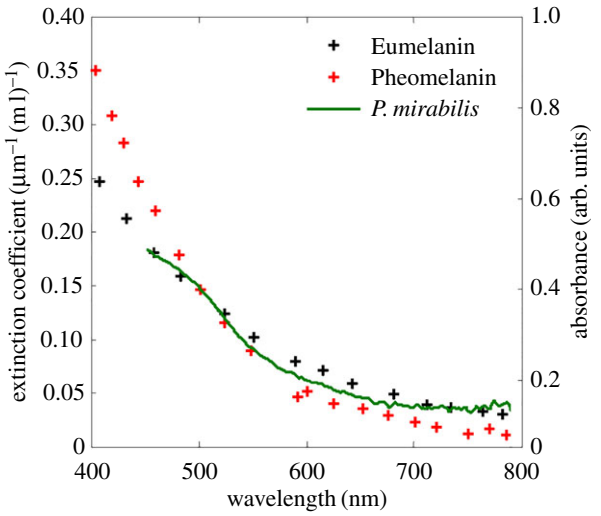

Figure 3. Measured absorbance spectra taken through the copper-gold coloured region of the *Pseudolestes mirabilis* hindwing membrane (plotted in arbitrary units) alongside the extinction coefficient of eumelanin and pheomelanin presented in Stavenga *et al*. (2012) [48] for comparison.

polarization-dependence of the reflectance as was measured experimentally (figure 2). Additionally, the modelling shows the reflectance depends strongly on the filling fraction. The filling fraction for optimal scattering leading to highest scattered intensities was found to be 45% material. Using image analysis software, the filling fraction of the actual *P. mirabilis* structure was calculated, across the FIB-milled sample regions imaged, to vary between 51% and 57% material.

In highly scattering systems scattering efficiency fundamentally depends on refractive index. To this end we also investigated the effect of varying the constituent refractive index of this structure by modelling its scattering of unpolarized incident light where the refractive index of the *P. mirabilis* system's fibre material was varied from $n = 1.0–2.7$; the complimentary space, between the fibres, was air. Figure 4*d* shows that higher refractive indices of the material give a stronger average reflectance, up to 82% when the refractive index of the fibre reaches 2.7 (i.e. close to that of rutile titanium dioxide, a synthetic dielectric material commonly used in broadband scattering systems). In addition, we also observe that the optimum filling-fraction for higher refractive index fibres, namely that which incurs the highest scattering efficiency, is lower than it is for fibres comprising lower refractive index. Interestingly, models of this system comprising a higher refractive index contrast show a significantly reduced degree of polarization (figure 4*e*).

4. Discussion

The damselfly *P. mirabilis* is endemic to Hainan Island, China, and is the only known representative of its family, *Pseudolestidae*, which is at present of uncertain affinity [49]. It frequents small, clear, well-lit forest streams. Males perch with wings held flat in an arrow-head posture on vegetation in sunspots where males defend territories for breeding purposes [44]. The hindwings of both sexes are broad, short and falcate, and are proportionally much shorter than the forewing than in other odonates.

The brilliant white reflection from the wing-underside of male *P. mirabilis* damselflies is used in signalling during territorial disputes, in which two protagonists face each other in a protracted hovering display, from 10–20 cm apart (figure 1*a*), which may last five minutes or more [44]. Generally the short falcate hindwings bearing the reflective fibres are held motionless and folded downward under the insect, with occasional flaps in which the white underside is vividly displayed. The degree of white reflection varies with maturity (the specimens analysed being fully mature), as in young males the reflective fibres are less developed in both density and extent, and are entirely absent in pre-reproductive teneral specimens [45]. Therefore, the brightness and extent of the underside white area may well serve as an indicator of a male's maturity and general fitness. In the hindwing the reflective wax is estimated to add about 20% to total wing mass in mature specimens [45], which must increase the effort required to flap the wings, as is suggested by studies on the flight kinematics of *Neurobasis chinensis* (Linnaeus, 1758), another species in which the hindwing is loaded [50,51], hence the frequency and vigour with which the white patches are flashed probably conveys further information on the fitness of the displaying male. This information may also provide a basis for female choice, as contests often occur in the presence of potential mates (G. T. Reels, personal communication). The filaments appear to be a secretion, rather than an outgrowth of the epicuticle, as they shear off easily from the secretory face of the veins. The standard model of the insect cuticle provides a ready explanation for their origin. In all insects wax canals traverse the epicuticle and secrete a surface deposit of wax [52]. In Odonata secretion of wax on the body and wings is believed to be often especially copious and to occur throughout life [43,46], but the form this takes in *P. mirabilis* is unique [45].

The optical structure is also visible on the wing-upperside, filtered through a tinted membrane to produce a brilliant copper-gold effect. This is displayed when the male is perched in its characteristic posture, typically horizontally on a leaf in full sunlight with hindwings held flat and swept back in an arrow-head shape (electronic supplementary material, 2), and makes the insect passively guarding its territory highly conspicuous, especially against green vegetation (this is a human perception, but current knowledge of odonate colour vision suggests it is likely to be true also for *P. mirabilis* [53,54]). In this case the very broad angle over which light is scattered from the underlying optical structure allows the bright colour filtered through the tinted wing membrane to be perceived by approaching conspecifics from a large overhead solid angle and might alternatively, discourage other males from attempting to set up residence, or may attract females, although there is no clear evidence of courtship behaviour [41]. The structure must be produced at considerable material cost, and presumably also encumbers the male considerably, hence it is surely the result of strong selective pressure.

Several other examples of structural whiteness in nature include photonic structures for which there are both fully optimized and un-optimized examples [35]. Despite the fact that the *P. mirabilis* photonic structure is not perfectly optimized with respect to its filling fraction, it is still an impressively efficient scattering medium. The reflectance properties of *P. mirabilis* are similar to those measured from several species of white beetle [35,36] whose reflective scattering efficiency compares favourably to paper (single-sheet, 80 gsm) and polystyrene. It was found that despite even the thickest of the three beetle scales having a cross-section

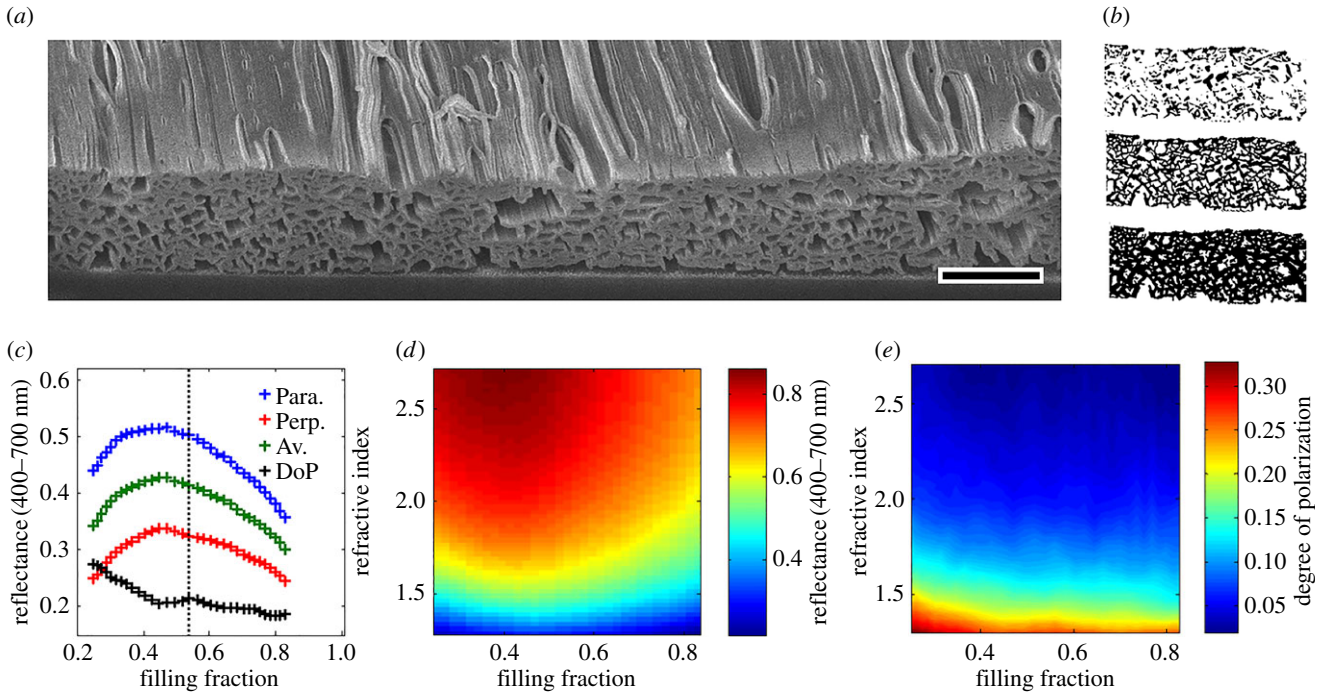

Figure 4. (*a*) SEM image of a cross-section through the *Pseudolestes mirabilis* photonic structure, revealing the disordered geometries present. (*b*) Example regions from model-structures with material filling fractions of 25%, 54% and 83%. (*c*) Graph showing the calculated reflectance (averaged over a wavelength-range of 400–700 nm) as a function of the filling fraction for both polarization states (blue markers show parallel polarization reflectance; green markers show perpendicular polarization reflectance) and the corresponding degree of polarization for each filling fraction (black markers). (*d*) Colour-map showing the average reflectance for unpolarized light as a function of filling fraction and material refractive index. (*e*) Colour-map showing the degree of polarization as a function of filling fraction and refractive index. Scale bar in (*a*) is 5 µm.

thickness of less than a tenth of a standard sheet of paper, the enhanced scattering from the disordered inter-scale structures yielded similar optical properties. The measured reflectance of *P. mirabilis* is comparable to that of the beetle *Lepidopta stigma*, whereas in *Cyphochilus* species and *Calothyrza margaritifera*, in which the optical scattering structures are more fully optimized, the reflectance is approximately 10% greater in intensity [35]. More recently, these structures have been shown to possess the lowest transport mean free path reported to date for low-refractive-index systems [36].

This system may be the first example of a brilliant white biological system that exhibits a discernible measured linear polarization-dependent response. This type of polarization signature is normally associated with more highly ordered structures, such as two-dimensional photonic crystals [55]. In biological systems, this two-dimensional order has been investigated in several species, the most common example of which is the male peacock, whose well-known, bright feather colours are produced by a system of two-dimensional photonic crystal domains of melanin rods packed into its feather barbules [56,57]. This also produces polarization-dependent saturated colour reflectance. The colour of the polychaete worm, *Pherusa*, is also known to arise from hexagonally two-dimensional ordered and quasi-ordered arrangements of cylindrical channels [58]; a similar structure exists also in the sea mouse *Aphrodita* [59,60]. The structure of the wax filaments comprising the white patches of the *P. mirabilis* ventral hindwing surface, combined with a separate absorbing filter on the upperside, represents an efficient method to create two quite separate visual signals from the same photonic structure. It is also a template for the design of a brilliant white system that possesses a linear polarization signature. Polarization signatures and white appearances are two optical properties normally not associated with one another. It is unclear, however, if differential linear polarization scatter serves a biological function in this species or is purely an incidental property of the packed filament structure that evolved in response to selection for an intense white signal. The 'arrowhead' perching posture (electronic supplementary material, 2) is unique among extant Odonata, and may well be a response to optimize the optical signal broadcast, given the differential scatter along the wing axes. It is well known that odonates can perceive polarized light [61,62] and perhaps even a small contrast between the two wings may enhance the overall signal received. However, field tests are needed to establish this hypothesis.

Authors' contributions. All authors contributed to the research and wrote the paper.

Data accessibility. All data needed to evaluate the conclusions in the paper are present in the paper and the electronic supplementary materials.

Competing interests. We declare we have no competing interests.

Funding. We acknowledge the financial support of AFOSR grant no. FA9550-10-1-0020.

Acknowledgements. The authors thank Graham Reels for providing the photographs of a *Pseudolestes mirabilis* damselfly in flight and specimens for this study and Haomiao Zhang for additional specimens to A.G.O. Both also generously shared their field observations of the insect. We thank Luke McDonald for assistance with scatterometry measurements; Stephen Luke for useful discussions; and Tim Starkey, Bodo Wilts and Doekele Stavenga for critical reading and discussion of the manuscript.

References

1. Fox DL. 1976 *Animal biochromes and structural colours: physical, chemical, distributional & physiological features of coloured bodies in the animal world*. Oakland, CA: University of California Press.
2. Srinivasarao M. 1999 Nano-optics in the biological world: beetles, butterflies, birds, and moths. *Chem. Rev.* **99**, 1935–1962. (doi:10.1021/cr970080y)
3. Vukusic P, Sambles JR. 2003 Photonic structures in biology. *Nature* **424**, 852–855. (doi:10.1038/nature01941)
4. Kinoshita S. 2013 *Bionanophotonics: an introductory textbook*. Singapore: Pan Stanford Publishing.
5. Starkey T, Vukusic P. 2013 Light manipulation principles in biological photonic systems. *Nanophotonics* **2**, 289–307. (doi:10.1515/nanoph-2013-0015)
6. Vignolini S, Rudall PJ, Rowland AV, Reed A, Moyroud E, Faden RB, Baumberg JJ, Glover BJ, Steiner U. 2012 Pointillist structural color in Pollia fruit. *Proc. Natl Acad. Sci. USA* **109**, 15 712–15 715. (doi:10.1073/pnas.1210105109)
7. Biro, LP, Vigneron, JP. 2011 Photonic nanoarchitectures in butterflies and beetles: valuable sources for bioinspiration. *Laser Photon. Rev.* **5**, 27–51. (doi:10.1002/lpor.200900018)
8. Loyau A, Gomez D, Moureau B, Thery M, Hart NS, Jalme MS, Bennett ATD, Sorci G. 2007 Iridescent structurally based coloration of eyespots correlates with mating success in the peacock. *Behav. Ecol.* **18**, 1123–1131. (doi:10.1093/beheco/arm088)
9. Stavenga DG, Leertouwer HL, Marshall NJ, Osorio D. 2010 Dramatic colour changes in a bird of paradise caused by uniquely structured breast feather barbules. *Proc. R. Soc. B* **278**, 2098–2104. (doi:10.1098/rspb.2010.2293)
10. Mathger LM, Hanlon RT. 2006 Anatomical basis for camouflaged polarized light communication in squid. *Biol. Lett.* **2**, 494–496. (doi:10.1098/rsbl.2006.0542)
11. Wilts BD, Pirih P, Arikawa K, Stavenga DG. 2013 Shiny wing scales cause spec(tac)ular camouflage of the angled sunbeam butterfly, *Curetis acuta*. *Biol. J. Linn. Soc.* **109**, 279–289. (doi:10.1111/bij.12070)
12. Ghiradella H. 1984 Structure of iridescent Lepidopteran scales: variations on several themes. *Ann. Entomol. Soc. Am.* **77**, 637–645. (doi:10.1093/aesa/77.6.637)
13. Vukusic P, Sambles JR, Lawrence CR, Wootton RJ. 1999 Quantified interference and diffraction in single *Morpho* butterfly scales. *Proc. R. Soc. Lond. B* **266**, 1403–1411. (doi:10.1098/rspb.1999.0794)
14. Kinoshita S, Yoshioka S, Fujii Y, Okamoto N. 2002 Photophysics of structural color in the morpho butterflies. *Forma* **17**, 103–121.
15. Hariyama T, Hironaka M, Horiguchi H, Stavenga DG. 2005 The leaf beetle, the jewel beetle, and the damselfly; insects with a multilayered show case. In *Structural colours in biological systems—principles and applications* (eds S Kinoshita, S Yoshioka). Osaka, Japan: Osaka University Press.
16. Noyes JA, Vukusic P, Hooper IR. 2007 Experimental method for reliably establishing the refractive index of buprestid beetle exocuticle. *Opt. Express* **15**, 4351. (doi:10.1364/OE.15.004351)
17. Stavenga DG, Wilts BD, Leertouwer HL, Hariyama T. 2011 Polarized iridescence of the multilayered elytra of the Japanese jewel beetle, Chrysochroa fulgidissima. *Phil. Trans. R. Soc. B* **366**, 709–723. (doi:10.1098/rstb.2010.0197)
18. Neville AC, Caveney S. 1969 Scarabaeid beetle exocuticle as an optical analogue of cholesteric liquid crystals. *Biol. Rev.* **44**, 531–562. (doi:10.1111/j.1469-185X.1969.tb00611.x)
19. Goldstein DH. 2005 Reflection properties of Scarabaeidae. Polarization Science and Remote Sensing II, 58880T. (http://dx.doi.org/10.1117/12.618546)
20. Jewell SA, Vukusic P, Roberts NW. 2007 Circularly polarized colour reflection from helicoidal structures in the beetle *Plusiotis boucardi*. *New J. Phys.* **9**, 99. (doi:10.1088/1367-2630/9/4/099)
21. Sharma V, Crne M, Park JO, Srinivasarao M. 2009 Structural origin of circularly polarized iridescence in jeweled beetles. *Science* **325**, 449–451. (doi:10.1126/science.1172051)
22. Schröder-Turk GE, Wickham S, Averdunk H, Brink F, Fitz Gerald JD, Poladian L, Large MCJ, Hyde ST. 2011 The chiral structure of porous chitin within the wing-scales of *Callophrys rubi*. *J. Struct. Biol.* **174**, 290–295. (doi:10.1016/j.jsb.2011.01.004)
23. Poladian L, Wickham S, Lee K, Large MC. 2008 Iridescence from photonic crystals and its suppression in butterfly scales. *J. R. Soc. Interface* **6**, S233–S242. (doi:10.1098/rsif.2008.0353.focus)
24. Wilts BD, Michielsen K, De Raedt H, Stavenga DG. 2011 Iridescence and spectral filtering of the gyroid-type photonic crystals in *Parides sesostris* wing scales. *Interface Focus* **2**, 681–687. (doi:10.1098/rsfs.2011.0082)
25. Yoshioka S, Fujita H, Kinoshita S, Matsuhana B. 2013 Alignment of crystal orientations of the multi-domain photonic crystals in *Parides sesostris* wing scales. *J. R. Soc. Interface* **11**, 20131029. (doi:10.1098/rsif.2013.1029)
26. Fitzstephens DM, Getty T. 2000 Colour, fat and social status in male damselflies, *Calopteryx maculata*. *Anim. Behav.* **60**, 851–855. (doi:10.1006/anbe.2000.1548)
27. Vukusic P, Wootton RJ, Sambles JR. 2004 Remarkable iridescence in the hindwings of the damselfly *Neurobasis chinensis chinensis* (Linnaeus) (Zygoptera: Calopterygidae). *Proc. R. Soc. Lond. B* **271**, 595–601. (doi:10.1098/rspb.2003.2595)
28. Schultz TD, Fincke OM. 2009 Structural colours create a flashing cue for sexual recognition and male quality in a Neotropical giant damselfly. *Funct. Ecol.* **23**, 724–732. (doi:10.1111/j.1365-2435.2009.01584.x)
29. Nixon MR, Orr AG, Vukusic P. 2013 Subtle design changes control the difference in colour reflection from the dorsal and ventral wing-membrane surfaces of the damselfly *Matronoides cyaneipennis*. *Opt. Express* **21**, 1479. (doi:10.1364/OE.21.001479)
30. Nixon MR, Orr AG, Vukusic P. 2015 Wrinkles enhance the diffuse reflection from the dragonfly *Rhyothemis resplendens*. *J. R. Soc. Interface* **12**, 20140749. (doi:10.1098/rsif.2014.0749)
31. Guillermo-Ferreira R, Bispo PC, Appel E, Kovalev A, Gorb SN. 2015 Mechanism of the wing colouration in the dragonfly *Zenithoptera lanei* (Odonata: Libellulidae) and its role in intraspecific communication. *J. Insect Physiol.* **81**, 129–136. (doi:10.1016/j.jinsphys.2015.07.010)
32. Prum RO, Cole JA, Torres RH. 2004 Blue integumentary structural colours in dragonflies (Odonata) are not produced by incoherent Tyndall scattering. *J. Exp. Biol.* **207**, 3999–4009. (doi:10.1242/jeb.01240)
33. Gorb SN. 1995 Scanning electron microscopy of pruinosity in Odonata. *Odonatologica* **24**, 225–228.
34. Vukusic P, Hallam B, Noyes J. 2007 Brilliant whiteness in ultrathin beetle scales. *Science* **315**, 348. (doi:10.1126/science.1134666)
35. Luke SM, Hallam BT, Vukusic P. 2010 Structural optimization for broadband scattering in several ultra-thin white beetle scales. *Appl. Opt.* **49**, 4246. (doi:10.1364/AO.49.004246)
36. Burresi M, Cortese L, Pattelli L, Kolle M, Vukusic P, Wiersma DS, Steiner U, Vignolini S. 2014 Bright-white beetle scales optimise multiple scattering of light. *Sci. Rep.* **4**, 6075. (doi:10.1038/srep06075)
37. Stavenga DG, Stowe S, Siebke K, Zeil J, Arikawa K. 2004 Butterfly wing colours: scale beads make white pierid wings brighter. *Proc. R. Soc. Lond. B* **271**, 1577–1584. (doi:10.1098/rspb.2004.2781)
38. Luke SM, Vukusic P, Hallam B. 2009 Measuring and modelling optical scattering and the colour quality of white pierid butterfly scales. *Opt. Express* **17**, 14729. (doi:10.1364/OE.17.014729)
39. Levy-Lior A, Shimoni E, Schwartz O, Gavish-Regev E, Oron D, Oxford G, Weiner S, Addadi L. 2010 Guanine-based biogenic photonic-crystal arrays in fish and spiders. *Adv. Funct. Mater.* **20**, 320–329. (doi:10.1002/adfm.200901437)
40. Mäthger LM *et al.* 2013 Bright white scattering from protein spheres in color changing, flexible cuttlefish skin. *Adv. Funct. Mater.* **23**, 3980–3989. (doi:10.1002/adfm.201203705)
41. Stavenga DG, Leertouwer HL, Pirih P, Wehling MF. 2009 Imaging scatterometry of butterfly wing scales. *Opt. Express* **17**, 193. (doi:10.1364/OE.17.000193)
42. Vukusic P, Stavenga D. 2009 Physical methods for investigating structural colours in biological systems. *J. R. Soc. Interface* **6**, S133–S148. (doi:10.1098/rsif.2008.0386.focus)
43. Hooper IR, Vukusic P, Wootton RJ. 2006 Detailed optical study of the transparent wing membranes of

the dragonfly *Aeshna cyanea*. *Opt. Express* **14**, 4891. (doi:10.1364/OE.14.004891)

44. Reels G. 2008 The phoenix damselfly (*Pseudolestes mirabilis*) of Hainan Island, China. *Agrion* **12**, 44–45.
45. Orr AG, Nixon MR, Vukusic P. 2017 The nature and structure of the white-reflecting underside 'scales' on the hindwing of *Pseudolestes mirabilis* Kirby (Zygoptera: Pseudolestidae). *Odonatologica*. In Press.
46. Gorb S., Kesel A, Berger J. 2000 Microsculpture of the wing surface in Odonata: evidence for cuticular wax covering. *Arthropod Struct. Dev.* **29**, 129–135. (doi:10.1016/S1467-8039(00)00020-7)
47. Gorb SN, Tynkkynen K, Kotiaho JS. 2009 Crystalline wax coverage of the imaginal cuticle in Calopteryx splendens (Odonata: Calopterygidae). *Int. J. Odonatol.* **12**, 201–221. (doi:10.1080/13887890.2009.9748340)
48. Stavenga DG, Leertouwer HL, Hariyama T, De Raedt HA, Wilts BD. 2012 Sexual dichromatism of the damselfly *Calopteryx japonica* caused by a melanin-chitin multilayer in the male wing veins. *PLoS ONE* **7**, e49743. (doi:10.1371/journal.pone.0049743)
49. Dijkstra KDB, Kalkman VJ, Dow RA, Stokvis FR, Van Tol J. 2013 Redefining the damselfly families: a comprehensive molecular phylogeny of Zygoptera (Odonata). *Syst. Entomol.* **39**, 68–96. (doi:10.1111/syen.12035)
50. Günther A, Hilfert-Rüppell D, Rüppell G. 2014 Reproductive behaviour and the system of signalling in *Neurobasis chinensis*—a kinematic analysis. *Int. J. Odonatol.* **17**, 31–52. (doi:10.1080/13887890.2014.881305)
51. Orr AG, Hämäläinen M. 2007 *The metalwing demoiselles of the eastern tropics*. Kota Kinabalu, Borneo, Malaysia: Natural History Publications (Borneo).
52. Chapman RF. 1998 *The insects: structure and function*, 4th edn. Cambridge, UK: Cambridge University Press.
53. Briscoe AD, Chittka L. 2001 The evolution of colour vision in insects. *Annu. Rev. Entomol.* **46**, 471–510. (doi:10.1146/annurev.ento.46.1.471)
54. Futahashi R, Kawahara-miki R, Kinoshita M, Yoshitake K, Yajima S. 2015 Extraordinary diversity of visual opsin genes in dragonflies. *Proc. Natl Acad. Sci. USA* **112**, E1247–E1256. (doi:10.1073/pnas.1424670112)
55. Johnson SG, Mekis A, Fan S, Joannopoulos JD. 2001 Molding the flow of light. *Comput. Sci. Eng.* **3**, 38–47. (doi:10.1109/5992.963426)
56. Yoshioka S, Kinoshita S. 2002 Effect of macroscopic structure in iridescent color of the peacock feathers. *Forma* **17**, 169–181.
57. Zi J, Yu X, Li Y, Hu X, Xu C, Wang X, Liu X, Fu R. 2003 Coloration strategies in peacock feathers. *Proc. Natl Acad. Sci. USA* **100**, 12 576–12 578. (doi:10.1073/pnas.2133313100)
58. Trzeciak TM, Vukusic P. 2009 Photonic crystal fiber in the polychaete worm *Pherusa* sp. *Phys. Rev. E* **80**. (doi:10.1103/PhysRevE.80.061908)
59. Parker AR, Mcphedran RC, McKdnzie DR, Botten LC, Nicorovici N-AP. 2001 Aphrodite's iridescence. *Nature* **409**, 36–37. (doi:10.1038/35051168)
60. McPhedran R, Nicorovici N, McKenzie D, Rouse G, Botten L, Welch V, Parker A, Wohlgennant M, Vardeny V. 2003 Structural colours through photonic crystals. *Physica B Condens. Matter* **338**, 182–185. (doi:10.1016/S0921-4526(03)00483-6)
61. Wehner R, Labhart T. 2006 Polarisation vision, 291–348. In *Invertebrate vision*. (eds E Warrant, D-E Nilsson). Cambridge, UK: Cambridge University Press.
62. Bernáth B, Szedenics G, Wildermuth H, Horváth G. 2002 How can dragonflies discern bright and dark waters from a distance? The degree of polarisation of reflected light as a possible cue for dragonfly habitat selection. *Freshw. Biol.* **47**, 1707–1719. (doi:10.1046/j.1365-2427.2002.00931.x)